European Journal of Mechanics / A Solids 71 (2018) 394–403

Contents lists available at ScienceDirect

European Journal of Mechanics / A Solids

journal homepage: www.elsevier.com/locate/ejmsol

Response of an infinite beam on a bilinear elastic foundation: Bridging the gap between the Winkler and tensionless foundation models

Yin Zhang[a,b,*], Xiaoming Liu[a,b], Yujie Wei[a,b]

[a] State Key Laboratory of Nonlinear Mechanics (LNM), Institute of Mechanics, Chinese Academy of Sciences, Beijing 100190, China
[b] School of Engineering Science, University of Chinese Academy of Sciences, Beijing 100049, China

ARTICLE INFO

Keywords:
Beam
Winkler foundation
Tensionless foundation
Bilinear foundation

ABSTRACT

The response of an infinite beam on an elastic foundation depends on the property/modeling of the foundation. There is a qualitative difference between the responses of a beam when it is on the Winkler foundation and on the tensionless foundation. A bilinear elastic foundation model, which describes the different behaviors of the elastic foundation in the tensile and compressive zones with two different foundation moduli, is proposed and a straightforward computational method is also formulated. The Winkler and tensionless foundations are shown to be the two special cases of the bilinear elastic foundation model. With this bilinear elastic foundation model, a more general method of modeling an elastic foundation is provided, which can be of some help to the modeling of the support of the ballastless high-speed railway.

1. Introduction

Fig. 1(a) shows an infinite beam on an elastic foundation subjected to a concentrated load, which, for many years, has been an important model to analyze the deflections and stresses of a railroad track (Ang and Dai, 2013; Bian et al., 2014; Choros and Adams, 1979; Hetényi, 1946; Kerr, 1972, 1974; 1976; Lancioni and Lenci, 2010; Lin and Adams, 1987; Tran et al., 2014). In a regular ballasted railroad, the rail-tie frame is laid on a layer of crushed stone called ballast (Kerr, 1974). The rail actually lifts off its ballast in front of, and behind a moving train (Choros and Adams, 1979; Lin and Adams, 1987). Once the lift-off occurs, the ballast layer as an elastic foundation cannot exert any (tensile) force on the rail (Choros and Adams, 1979; Lin and Adams, 1987). While, the Winkler foundation model assumes that there is only one foundation modulus, which physically means that the Winkler foundation reacts the same in tension as in compression. Although nowadays the Winkler foundation model is still widely used to analyze the rail system (Ang and Dai, 2013; Tran et al., 2014), its usage is motivated more by the desire for mathematical simplicity than by physical reality (Lin and Adams, 1987). Therefore, the tensionless foundation model is more appropriate and often applied to study the contact between the rail and ballast (Choros and Adams, 1979; Lancioni and Lenci, 2010; Lin and Adams, 1987). The tensionless foundation is also called the foundation that reacts in compression only (Weitsman, 1970) or the unilateral springs/supports/foundation (Bhattiprolu et al., 2013, 2014; 2016; Dempsey et al., 1984; Lancioni and Lenci, 2010). Because there is no bonding force between a structure and the tensionless foundation, their contact is referred to as the unbonded contact (Weitsman, 1969); because a structure can separate/lift off the tensionless foundation, which results in a decreasing contact area, their contact is also referred to as the receding contact (Keer et al., 1972). However, when the tensionless foundation model is applied to the ballastless track system, which has been extensively used in the high-speed railway, a serious problem may arise: The ballastless railway support can take some tension (Bian et al., 2014). A ballastless high-speed railway consists of the following two parts (Bian et al., 2014): (1) the track superstructure (rail, fastener, track slab, cement asphalt mortar (CAM) layer and concrete base) and (2) the geotechnical substructure (roadbed, subgrade and subsoil). A major difference between the ballastless and ballasted tracks is the concrete track slabs replacing the ballast layer (Bian et al., 2014). The fasteners tightly bond the rail with track slab and the CAM layer bonds the track slab with the concrete base, which makes the rail separation from its support extremely difficult if there is any. Furthermore, the support capability of bearing tensile stress may become substantial because of the tight bondings between the rail/track slab, track slab/CAM and CAM/concrete base, etc. Actually, tensile stress was indeed detected by the sensors embedded in the roadbed layer underneath the concrete base (Bian et al., 2014). Recent elasticity analyses show that even for a homogeneous elastic continuum modeled as an elastic half-space, its surface responses to tension and compression are intrinsically different (Zhuo and Zhang, 2015a, 2015b). This asymmetric response to tension and compression is

* Corresponding author. State Key Laboratory of Nonlinear Mechanics (LNM), Institute of Mechanics, Chinese Academy of Sciences, Beijing 100190, China.
E-mail address: zhangyin@lnm.imech.ac.cn (Y. Zhang).

https://doi.org/10.1016/j.euromechsol.2018.06.006
Received 7 January 2018; Received in revised form 7 June 2018; Accepted 7 June 2018
Available online 15 June 2018
0997-7538/

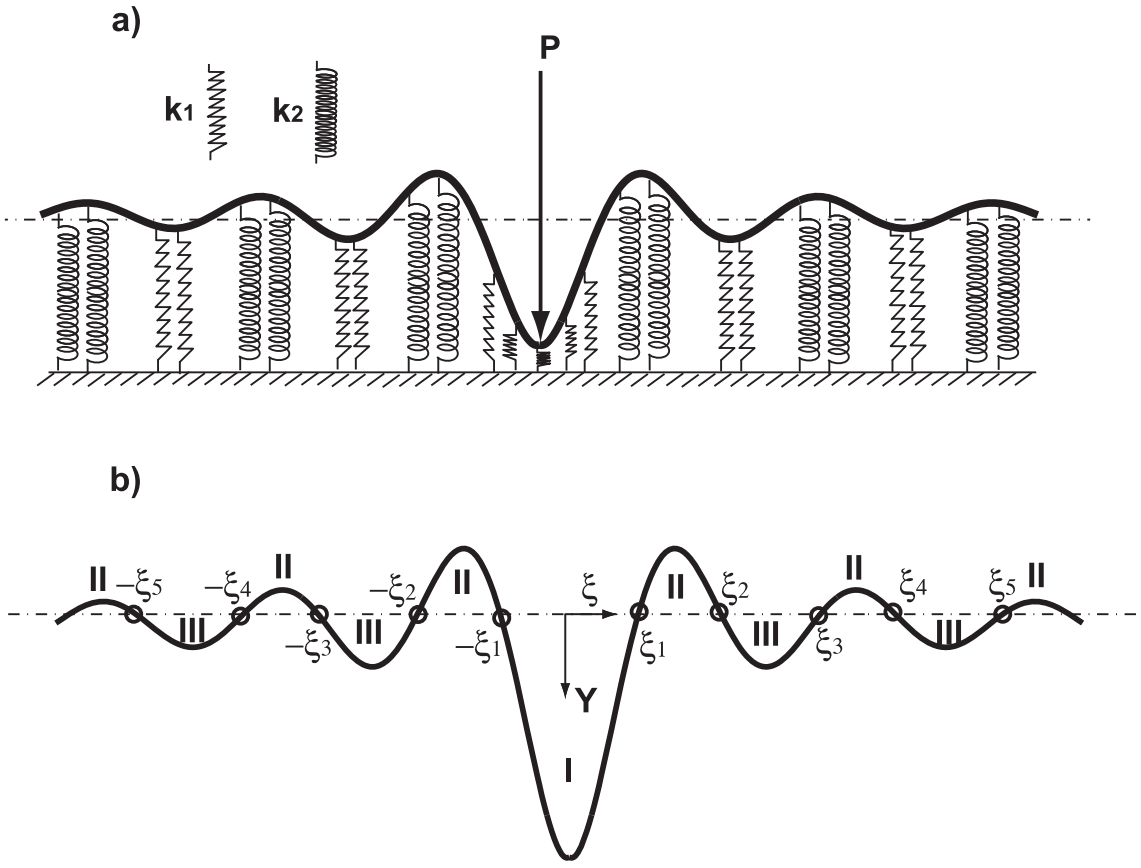

Fig. 1. (a) Schematic diagram of an infinite beam on a bilinear elastic foundation subjected to a concentrated load P. When the beam bends downwards/upwards, the foundation is with compression/tension and the corresponding foundation modulus is k_1/k_2. When $k_2 = 0$, the foundation is the tensionless foundation; when $k_2 = k_1$, it is the Winkler foundation. (b) The coordinate system and deflection areas. The zero points (ξ_i), which demarcate the areas, are marked with circles. Area **I** is the downward compressive deflection area with the concentrated load P and in comparison, area **III** is the other downward compressive deflection areas with no P. Area **II** are the upward tensile deflection areas.

also the mechanism responsible for the period-doubling behavior of the perfectly bonded film/substrate system in a post-buckling region (Brau et al., 2011). A bilinear elastic foundation model with two different foundation moduli of k_1 and k_2 as shown in Fig. 1(a) is thus proposed to model the different behaviors in the tensile and compressive zones. The bilinear behavior of the ballastless railway support is expected because of its heterogeneous multilayer structure and the interface properties. In this bilinear model, the Winkler foundation and the tensionless foundation are the two special cases of $k_2/k_1 = 1$ and $k_2/k_1 = 0$, respectively.

The contact mechanics of a beam on the tensionless foundation has been intensively studied for many years and various solution methods have also been developed. Although the Lagrange multiplier or penalty-based algorithms in several finite element analysis (FEA) commercial softwares are capable of modeling the unilateral constraint, the computational costs are very expensive in both storage and CPU time (Silveira et al., 2008). Furthermore, the complexity of the tools required to perform a comprehensive study or analyses such as design optimization, feedback control or stability etc can be infeasible for a full-scale FEA simulation (Attar et al., 2016; Silveira et al., 2008). There have always been interests to develope the methods to reduce the computational cost in an extensive parametric study of tensionless contact (Attar et al., 2016). A major difficulty in the tensionless contact problem is the unknown property of contact area, which makes the problem nonlinear and extremely difficult to be solved in some scenarios. Therefore, recent studies have been focusing on developing efficient methods of determining the contact area (Attar et al., 2016; Bhattiprolu et al., 2013, 2014; 2016; Ma et al., 2009a, 2009b; 2011; Nobili, 2013; Silveira et al., 2008). The incremental-iterative methods (Attar et al., 2016; Bhattiprolu et al., 2013; Silveira et al., 2008) update the governing equation/stiffness matrices in each iteration by tracking the structure deflections and continue until the convergence, which can still involve significant computation efforts. For example, a large number of modes (up to 20) in the Galerkin method are required to achieve a satisfying accuracy (Bhattiprolu et al., 2013). The transfer displacement function method (Ma et al., 2009a) reduces the computation by solving the contact/noncontact zones and deflections one by one. Besides, the tensionless contact properties can also be utilized to reduce the computational efforts. For example, there is an outstanding characteristics in the beam tensionless contact subjected to a concentrated load: Only one contact area exists for both the infinite (Tsai and Westmann, 1967; Weitsman, 1970, 1972) and finite (Zhang, 2008; Zhang and Murphy, 2004, 2013) beams. Even in the contact dynamics with a moving concentrated load, the one contact area conclusion still holds as far as the moving speed of the concentrated load is less than the critical speed of $\sqrt[4]{4EIk_1/m^2}$ (EI, m are the beam bending stiffness and mass per unit length) (Weitsman, 1971). It needs to keep in mind that under complex loads, the scenario of multiple contact areas can occur (Ma et al., 2009a, 2009b; 2011; Nobili, 2013). The zero points as called by Hetényi (1946) and shown in Fig. 1(b) are the points at which the beam deflection is zero. For the tensionless contact, the zero points are also the lift-off/separation points demarcating the contact areas (Weitsman, 1970). For an infinite beam, by reducing the two zero points to one via the symmetry property, the analytical (Weitsman, 1970) or approximate analytical solution (Weitsman, 1972) can be derived.

Compared with the abundant literature of the tensionless contact,

the studies on the bilinear foundation are few (Farshad and Shahinpoor, 1972; Shahwan and Waas, 1994). For the perturbation method developed by Farshad and Shahinpoor (1972) to work, the two foundation moduli, k_1 and k_2 must be close to each other. As the result, their perturbation method can only handle a very small k_2/k_1 range around $k_2/k_1 = 1$. Shahwan and Waas (1994) defined a force (f)-displacement (w) relation for a bilinear foundation as $f = k_1\Psi(w)$ and $\Psi(w) = w[1/2(1 - \tanh(\lambda w)]$. Here λ is the so-called foundation attachment coefficient; $\lambda = \infty$ corresponds to the fully unattached, i.e., tensionless foundation; when $\lambda = 0$, $\Psi(w) = 1/2w$ and this $1/2$ factor needs to be replaced by 1, which thus corresponds to the fully attached, i.e., Winkler foundation. However, firstly, the physical meaning of λ is not clear and it will be difficult to experimentally determine such a parameter. Secondly, large λ can cause "numerical difficulties" and unphysical results are thus obtained (Shahwan and Waas, 1994).

In contrast to the tensionless case, the zero point number of an infinite beam on the Winkler foundation is infinite (Hetényi, 1946). Therefore, before we can begin to determine the positions of the zero points, we firstly encounter the problem: How many zero points are there in a bilinear elastic foundation with a varying k_2/k_1? Besides the tensionless foundation property of one contact area as mentioned above, the Winkler foundation property of a rapid deflection decay from the concentrated load (Hetényi, 1946) is also noticed. In conjunction with these two properties, a computation method with the assumption of a few zero points is proposed, which can sufficiently capture the beam deflection around the loading point. Compared with the previous studies (Farshad and Shahinpoor, 1972; Shahwan and Waas, 1994), the computation proposed in this study is straightforward and capable of handling all the cases of k_2/k_1 varying from 0 to ∞. Its accuracy is also demonstrated. The zero points of the bilinear, Winkler and tensionless foundations are all shown to be independent on the magnitude of the concentrated load. The zero points are determined by the beam bending stiffness and foundation moduli only. The magnitude of the concentrated load only changes the deflection amplitude, which essentially means that only one computation is needed for the concentrated load scenario. This unique property can be of a significant help to the various stress and deflection analyses related with the wheel-track contact load, which is modeled as a concentrated load (Ang and Dai, 2013; Choros and Adams, 1979; Hetényi, 1946; Kerr, 1972; Lancioni and Lenci, 2010; Lin and Adams, 1987; Tran et al., 2014).

2. Model development

The governing equation for an infinite beam on the Winkler foundation subjected to a concentrated load is given as follows (Hetényi, 1946)

$$EI\frac{d^4y}{dx^4} + k_1 y = P\delta(x) \tag{1}$$

Where y, E and I are the beam deflection, Young's modulus and area moment of inertia, respectively. As seen in Fig. 1, P is the concentrated load acting on $x = 0$; $\delta(x)$ is the Dirac delta function and k_1 is the foundation modulus. As the beam bends upwards and downwards, the Winkler foundation assumes that the foundation is firmly attached to the beam. As a result, the foundation experiences the tensile and compressive forces in different zones. The Winkler foundation model also assumes that the same foundation modulus, k_1, applies to both tensile and compressive zones. Furthermore, there is only normal pressure in the Winkler foundation. In order to include the effect of shear stress, the Pasternak foundation (Ebrahimi and Barati, 2017; Ebrahimi and Shaffiei, 2017) or the Reissner foundation (Kerr, 1964) model should be used.

The governing equation for the tensionless foundation is the following

$$\begin{cases} EI\frac{d^4y_1}{dx^4} + k_1 y_1 = P\delta(x), \ \left|x\right| \le x_1, \ y_1 \ge 0 \\ EI\frac{d^4y_2}{dx^4} = 0, \ \left|x\right| \ge x_1, \ y_2 \le 0. \end{cases} \tag{2}$$

The governing domains of the above two equations are demarcated by x_1, at which the beam lifts-off, or say, separates from the foundation. Unlike the Winkler foundation, the tensionless foundation can only exert compressive force on the beam; once the beam bends upwards, the force exerted by the foundation becomes zero, which is the physical meaning of the two equations in Eq. (2).

For the bilinear foundation, the governing equation becomes the following three

$$\begin{cases} EI\frac{d^4y_1}{dx^4} + k_1 y_1 = P\delta(x), \ \mathbf{I}, \ y_1 \ge 0 \\ EI\frac{d^4y_2}{dx^4} + k_2 y_2 = 0, \ \mathbf{II}, \ y_2 \le 0 \\ EI\frac{d^4y_3}{dx^4} + k_1 y_3 = 0, \ \mathbf{III}, \ y_3 \ge 0. \end{cases} \tag{3}$$

In Eq. (3), there are two foundation moduli of k_1 and k_2, which indicate the different responses of bilinear foundation in the compressive and tensile zones. Physically, when $k_1 = k_2$, the bilinear foundation becomes the Winkler foundation and it becomes the tensionless foundation when $k_2 = 0$. The governing domains of the three equations are defined as area **I**, **II** and **III** as seen in Fig. 1(b).

The following quantities are introduced to nondimensionalize the above equations (Weitsman, 1970)

$$\xi = \beta x, \ \xi_i = \beta x_i, \ Y = \beta y, \ Y_i = \beta y_i, \ F = \frac{P}{4\beta^2 EI}, \ R = \sqrt[4]{\frac{k_2}{k_1}}, \ \beta = \sqrt[4]{\frac{k_1}{4EI}}. \tag{4}$$

Where β^{-1} is called "fundamental length" (Biot, 1937), which characterizes the important features of both the statics (Hetényi, 1946) and dynamics (Kerr, 1972) of a beam on an elastic foundation. As seen in Fig. 1(b), ξ_i s are the dimensionless zero points, which separate the tensile and compressive zones. Eqs. (1)–(3) are now nondimensionalized as follows

$$\frac{1}{4}Y'''' + Y = F\delta(\xi), \tag{5}$$

$$\begin{cases} \frac{1}{4}Y_1'''' + Y_1 = F\delta(\xi), \ |\xi| \le \xi_1, \ Y_1 \ge 0 \\ \frac{1}{4}Y_2'''' = 0, \ |\xi| \ge \xi_1, \ Y_2 \le 0. \end{cases} \tag{6}$$

and

$$\begin{cases} \frac{1}{4}Y_1'''' + Y_1 = F\delta(\xi), \ \mathbf{I}, \ Y_1 \ge 0 \\ \frac{1}{4}Y_2'''' + R^4 Y_2 = 0, \ \mathbf{II}, \ Y_2 \le 0 \\ \frac{1}{4}Y_3'''' + Y_3 = 0, \ \mathbf{III}, \ Y_3 \ge 0. \end{cases} \tag{7}$$

Here $()'''' = d^4/d\xi^4$. The analytical solution to Eq. (5) of the Winkler foundation was derived by Hetényi (1946), which is a symmetric one and the $\xi \ge 0$ part solution is given as follows

$$Y(\xi) = \frac{F}{2}e^{-\xi}(\sin\xi + \cos\xi), \ \xi \ge 0. \tag{8}$$

Several characteristics can be summarized from the above solution form: (1) $\lim_{\xi\to\infty} Y(\xi) = 0$. (2) It has the features of damped waves decaying with $e^{-\xi}$. As defined in Eq. (4), $\xi = \beta x$ and this length β^{-1} is thus often referred to as the (spatial) damping factor (Hetényi, 1946). (3) There are infinite zero points as determined by $\sin\xi + \cos\xi = 0$, which leads to $\xi_i = 3\pi/4 + (i - 1)\pi$. (4) The concentrated load (F) has no impact on the zero points. (5) The maximum beam deflection is $Y(0) = F/2$.

The solution form to Eq. (6) of the tensionless foundation was given

by Weitsman (1970) as follows:

$$\begin{cases} Y_1 = A_1 \sinh\xi \sin\xi + B_1 \cosh\xi \cos\xi - \frac{F}{2}\sinh|\xi|\cos\xi \\ \quad + \frac{F}{2}\cosh\xi \sin|\xi|, \ |\xi| \le \xi_1, \ Y_1 \ge 0 \\ Y_2 = A_2\xi^3 + B_2\xi^2 + C_2\xi + D_2, \ |\xi| \ge \xi_1, \ Y_2 \le 0. \end{cases} \tag{9}$$

The first two terms of Y_1 are the homogeneous solution and the last two are the particular solution. It is noticed that all four terms are even functions, which physically keep the solution symmetric. In the homogeneous solution, there are two other terms associated with the $\cosh\xi\sin\xi$ and $\cosh\xi\sin\xi$, which are thrown away because they are odd functions and thus violate the symmetry (Weitsman, 1970). Here A_1, B_1, A_2, B_2, C_2 and D_2 are the six constants to be determined. Besides these six unknown constants, the zero point ξ_1, which is variously referred to as the separation point (Weitsman, 1970), lift-off point (Zhang and Murphy, 2004) or touch-down point (Lancioni and Lenci, 2010), is also unknown. Although the two governing equations in Eq. (2) are individually linear, the tensionless contact problem as a whole is a nonlinear one because of the unknown property of the separation point(s), which is also the major computation difficulty encountered in various tensionless contact problems. At ξ_1, the transversality conditions (Kerr, 1976), which are also called the matching conditions (Zhang and Murphy, 2004) or the continuity conditions (Bhattiprolu et al., 2014, 2016), yield the following four equations:

$$Y_1(\xi_1) = Y_2(\xi_1), \ Y_1'(\xi_1) = Y_2'(\xi_1), \ Y_1''(\xi_1) = Y_2''(\xi_1), \ Y_1'''(\xi_1) = Y_2'''(\xi_1). \tag{10}$$

Physically, the above transversality conditions ensure the continuity of the beam deflection, slope, moment and shear force at $\xi = \xi_1$ (Zhang and Murphy, 2004). The boundary conditions require the vanishing deflection, moment and shear force at $\xi = \xi_1$ (Weitsman, 1970), which gives the following three equations:

$$Y_1(\xi_1) = 0, \ Y_1''(\xi_1) = 0, \ Y_1'''(\xi_1) = 0. \tag{11}$$

Because of Eq. (10), the above boundary conditions can also be equivalently written as $Y_2(\xi_1) = Y_2''(\xi_1) = Y_2'''(\xi_1) = 0$. Eqs. (10) and (11) provide seven equations in total to solve the seven unknowns of A_1, B_1, A_2, B_2, C_2, D_2 and ξ_1. For brevity, the lengthy derivation is omitted here and the solution is given as follows:

$$\begin{cases} Y_1 = \frac{F}{2}\Big(-\coth\frac{\pi}{2}\sinh\xi \sin\xi + \coth\frac{\pi}{2}\cosh\xi\cos\xi - \sinh|\xi|\cos\xi \\ \quad + \cosh\xi\sin|\xi|\Big), \ \Big|\xi\Big| \le \frac{\pi}{2}, \ Y_1 \ge 0 \\ Y_2 = \frac{F}{\sinh(\pi/2)}\Big(-|\xi| + \frac{\pi}{2}\Big), \ \Big|\xi\Big| \le \frac{\pi}{2}, \ Y_2 \le 0. \end{cases} \tag{12}$$

The above solution is also a symmetric one. Similarly, several characteristics about the tensionless contact are summarized as follows: (1) $\lim_{|\xi|\to\infty} Y_2(\xi) = \infty$ in contrast to $Y(\infty) = 0$ of the Winkler foundation. (2) The beam deflection of the detachment part is linear, which means that the beam bending generates no moment and force. Therefore, this linear beam deflection of the detachment, which can be infinitely large, actually does not violate the equilibrium. The concentrated load is balanced by the contact area alone. It is emphasized that only the infinite beam has this linear deflection of the detachment part. For a finite beam, only the free-free finite beam resembles this scenario and all other do not (Zhang and Murphy, 2004). (3) There are only two zero points of $\pm\xi_1 = \pi/2$ and therefore, there is only one contact area of $-\pi/2 \le \xi \le \pi/2$. Compared with that of the Winkler foundation, ξ_1 of the tensionless foundation is 33.3% smaller. (5) The concentrated load (F) has no impact on the zero point. (6) The maximum beam deflection is $Y_1(0) = F\coth(\pi/2)/2 \approx 1.09F/2$, which is 9% larger than that of the Winkler foundation. The above characteristics of the Winkler and tensionless foundations are also graphically illustrated in Fig. 2.

The solutions to Eq. (7) of the bilinear foundation are also symmetric. Therefore, only the solution forms of the $\xi > 0$ part are given as follows:

$$\begin{cases} Y_1 = A_1 \sinh\xi \sin\xi + B_1 \cosh\xi \cos\xi - \frac{F}{2}\sinh\xi\cos\xi \\ \quad + \frac{F}{2}\cosh\xi\sin\xi, \ I, \ Y_1 \ge 0 \\ Y_{2i} = A_{2i}e^{-R\xi}\sin(R\xi) + B_{2i}e^{-R\xi}\cos(R\xi) + C_{2i}e^{R\xi}\sin(R\xi) \\ \quad + D_{2i}e^{R\xi}\cos(R\xi), \ II_i, \ Y_2 \le 0 \\ Y_{3i} = A_{3i}e^{\xi}\sin\xi + B_{3i}e^{-\xi}\cos\xi + C_{3i}e^{\xi}\sin\xi + D_{3i}e^{\xi}\cos\xi, \ III_i, \ Y_3 \ge 0 \end{cases} \tag{13}$$

There are three domains of **I**, **II** and **III** for the three governing equations. Physically, area **I** is a special compressive zone within which the concentrated load is located and all other compressive zones are **III**; area **II** is the tensile zones. Here Y_{2i} and Y_{3i} are the solutions of area $\mathbf{II}_i$ and area $\mathbf{III}_i$, which are the ith tensile and compressive zones. For example, in Fig. 1(b) $\mathbf{II}_1$ is the area of $\xi_1 \le \xi \le \xi_2$ and $\mathbf{III}_1$ is that of $\xi_2 \le \xi \le \xi_3$.

Although the above solution forms are available for the bilinear foundation, the problem is still difficult because the positions of zero points and even their number are unknown. For the time being, we assume that there are only three zero points in the $\xi > 0$ region. From Eq. (13), we have the following:

$$\begin{cases} Y_1 = A_1\sinh\xi\sin\xi + B_1\cosh\xi\cos\xi - \frac{F}{2}\sinh\xi\cos\xi + \frac{F}{2}\cosh\xi\sin\xi, \ \mathbf{I} \\ \quad : 0 \le \xi \le \xi_1 \\ Y_{21} = A_{21}e^{-R\xi}\sin(R\xi) + B_{21}e^{-R\xi}\cos(R\xi) + C_{21}e^{R\xi}\sin(R\xi) \\ \quad + D_{21}e^{R\xi}\cos(R\xi), \ \mathbf{II}_1\text{: } \xi_1 \le \xi \le \xi_2 \\ Y_{31} = A_{31}e^{-\xi}\sin\xi + B_{31}e^{-\xi}\cos\xi + C_{31}e^{\xi}\sin\xi + D_{31}e^{\xi}\cos\xi, \ \mathbf{III}_1 \\ \quad : \xi_2 \le \xi \le \xi_3 \\ Y_{22} = A_{22}e^{-R\xi}\sin(R\xi) + B_{22}e^{-R\xi}\cos(R\xi)\mathbf{II}_2\text{: } \xi \ge \xi_3 \end{cases} \tag{14}$$

Notice that in the last equation of Eq. (14), area $\mathbf{II}_2$ governs the infinite region of $\xi \ge \xi_3$ because only three zero points are assumed. In order to have $\lim_{\xi\to\infty} Y_{22}(\xi) = 0$, the other two terms of $C_{22}e^{R\xi}\sin(R\xi)$ and $D_{22}e^{R\xi}\cos(R\xi)$ are discarded because either of them can make the beam deflection infinitely large. Now A_1, B_1, A_{21}, B_{21}, C_{21}, D_{21}, A_{31}, B_{31}, C_{31}, D_{31}, A_{22} and B_{22} plus the three zero points of ξ_1, ξ_2 and ξ_3 are fifteen unknowns in total. At each zero point, the same four transversality conditions as those in Eq. (10) are given. Therefore, the following twelve equations in total are given for three zero points

$$Y_1(\xi_1) = Y_{21}(\xi_1), \ Y_1'(\xi_1) = Y_{21}'(\xi_1), \ Y_1''(\xi_1) = Y_{21}''(\xi_1), \ Y_1'''(\xi_1) = Y_{21}'''(\xi_1)$$

$$Y_{21}(\xi_2) = Y_{31}(\xi_2), \ Y_{21}'(\xi_2) = Y_{31}'(\xi_2), \ Y_{21}''(\xi_2) = Y_{31}''(\xi_2), \ Y_{21}'''(\xi_2) = Y_{31}'''(\xi_2)$$

$$Y_{31}(\xi_3) = Y_{22}(\xi_3), \ Y_{31}'(\xi_3) = Y_{22}'(\xi_3), \ Y_{31}''(\xi_3) = Y_{22}''(\xi_3), \ Y_{31}'''(\xi_3) = Y_{22}'''(\xi_3) \tag{15}$$

There are also three constraint conditions defining the zero points (Zhang and Murphy, 2004), which are given as follows

$$Y_1(\xi_1) = 0, \ Y_{21}(\xi_2) = 0, \ Y_{31}(\xi_3) = 0. \tag{16}$$

Eqs. (15) and (16) provide fifteen equations in total. By substituting Eq. (14) into these fifteen equations, the fifteen unknowns can be solved by the Newton-Rhapson method (Press et al., 1986).

The previous tensionless contact study assumes only one contact area and thus only one zero point (Zhang and Murphy, 2004). In comparison, arbitrarily more zero points can be easily and systematically incorporated into the above computation formulation. For example, for the case of four zero points, Eq. (14) becomes the following

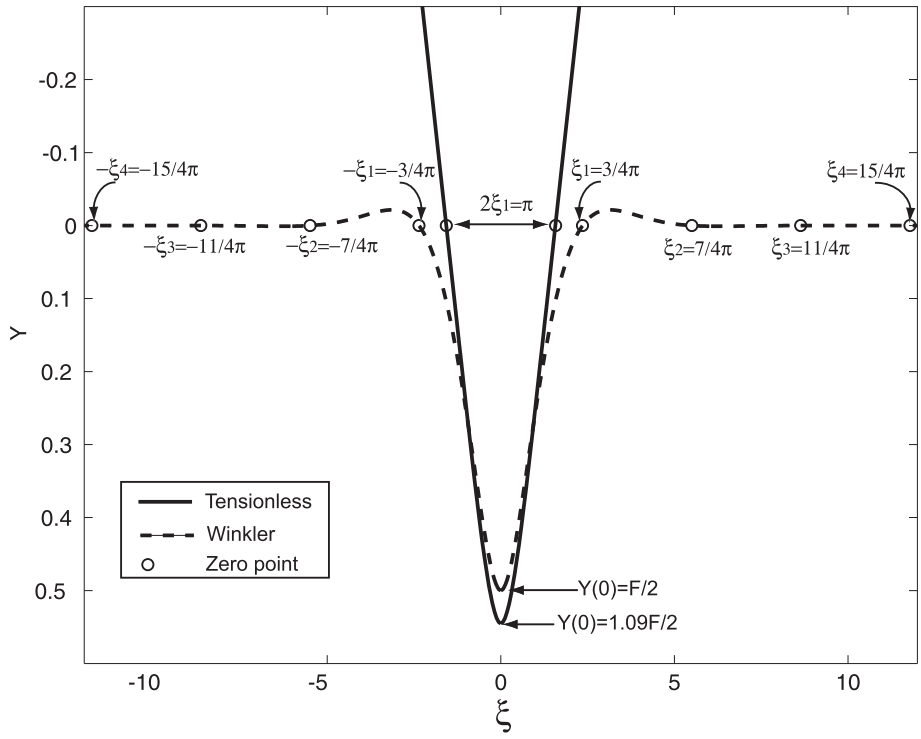

Fig. 2. Comparison of the beam deflections on the Winkler and tensionless foundations. For the tensionless foundation model, there is only one (downward) contact area and thus one zero point of $\xi_1 = \pi/2$ when $\xi > 0$. For the Winkler foundation model, there are infinite zero points given as $\xi_i = 3\pi/4 + (i-1)\pi$. At $\xi = 0$, the beam maximum deflections are $1.09F/2$ and $F/2$ for the tensionless and Winkler foundation models, respectively.

$$\begin{cases} Y_1 = A_1 \sinh\xi \sin\xi + B_1 \cosh\xi \cos\xi - \frac{F}{2}\sinh\xi\cos\xi + \frac{F}{2}\cosh\xi\sin\xi, \mathbf{I} \\ \quad : 0 \le \xi \le \xi_1 \\ Y_{21} = A_{21}e^{-R\xi}\sin(R\xi) + B_{21}e^{-R\xi}\cos(R\xi) + C_{21}e^{R\xi}\sin(R\xi) \\ \quad + D_{21}e^{R\xi}\cos(R\xi), \mathbf{II}_1: \xi_1 \le \xi \le \xi_2 \\ Y_{31} = A_{31}e^{-\xi}\sin\xi + B_{31}e^{-\xi}\cos\xi + C_{31}e^{\xi}\sin\xi + D_{31}e^{\xi}\cos\xi, \mathbf{III}_1 \\ \quad : \xi_2 \le \xi \le \xi_3 \\ Y_{22} = A_{22}e^{-R\xi}\sin(R\xi) + B_{22}e^{-R\xi}\cos(R\xi) + C_{22}e^{R\xi}\sin(R\xi) \\ \quad + D_{22}e^{R\xi}\cos(R\xi)\mathbf{II}_2: \xi_3 \le \xi \le \xi_4 \\ Y_{32} = A_{32}e^{-R\xi}\sin(R\xi) + B_{32}e^{-R\xi}\cos(R\xi)\mathbf{III}_2: \xi \ge \xi_4 \end{cases} \tag{17}$$

Compared with Eq. (14) of three zero-point case, there are five more unknowns: C_{22}, D_{22}, A_{32}, B_{32} and ξ_4. Therefore, there are twenty unknowns in total. The fifteen equations provided by Eqs. (15) and (16) are still applicable. At $\xi = \xi_4$, there are four more transversality conditions and one more constraint condition given as follows:

$$Y_{22}(\xi_4) = Y_{32}(\xi_4),\ Y_{22}^{'}(\xi_4) = Y_{32}^{'}(\xi_4),\ Y_{22}^{''}(\xi_4) = Y_{32}^{''}(\xi_4),\ Y_{22}^{'''}(\xi_4) = Y_{32}^{'''}(\xi_4);\ Y_{22}(\xi_4) = 0. \tag{18}$$

Similarly, by substituting Eq. (17) into the twenty equations of Eqs. (15), (16) and (18), the twenty unknowns can be solved by the Newton-Rhapson method. However, as discussed later in details, adding more zero points into the computation does not necessarily improve the accuracy. Fig. 3 shows the comparison between the analytical and numerical solutions for the Winkler foundation. The analytical solution is Eq. (8) and the numerical solution is Eq. (14) of three zero-point case by taking $R = 1$. The two curves almost overlap and their difference is extremely small. In the Winkler foundation case, though there are infinite zero points as seen in Eq. (8), the beam deflection decreases rapidly with an exponential decay of $e^{-\xi}$. As a result, the beam deflection away from the concentrated load is very small and thus has little contribution to the equilibrium. Therefore, the three zero-point configuration of the beam deflection can achieve a very accurate result because it captures the major deformations around the concentrated load.

3. Results and discussion

Before the results are presented, an important computational issue needs to be addressed. For Eq. (14) to be solved by the Newton-Rhapson method, an initial guess for the fifteen unknowns needs to be supplied for the program to start. A poor initial guess may result in the unwanted results or even no result at all for the Newton-Rhapson method (Press et al., 1986). By setting $R = 1$, the bilinear foundation starts with the Winkler foundation and the analytical solution of Eq. (8) can serve as a good guideline for a proper initial guess of the fifteen unknowns. By gradually changing R and using the previous computational results as the initial guess, the Newton-Rhapson method can smoothly run through a very large range of R. In the previous discussion, we reach the following conclusion: The concentrated load (F) has no influence on the zero points for both the Winkler foundation of Eq. (8) and the tensionless foundation of Eq. (12); the concentrated load acts as an amplification factor which modifies the deflection amplitude only. The above conclusion also applies to a finite beam on a tensionless foundation. Even the finite beam is subjected to an asymmetric concentrated load and with different boundary conditions, this conclusion holds as far as the beam length is relatively large (Zhang, 2008; Zhang and Murphy, 2004). For the bilinear foundation, our computations show that the same conclusion still applies. In all our computations, $F = 1$ is set.

Fig. 4 shows the three beam deflections with $k_2/k_1 = 1$, $k_2/k_1 = 10$ and $k_2/k_1 = 27102$. Here the $k_2/k_1 = 1$ case is the Winkler foundation. Their corresponding zero points of ξ_1s increase monotonically from $3\pi/4$ to 2.63 and to 3.06 as k_2/k_1 increases. Even with the significant variation of k_2/k_1, there is little change of the beam deflections around the center of area **I**. The major deflection changes occur around the edge of area **I** and in the tensile area of $\mathbf{II}_1$. Rapid decreases of the beam (upward)

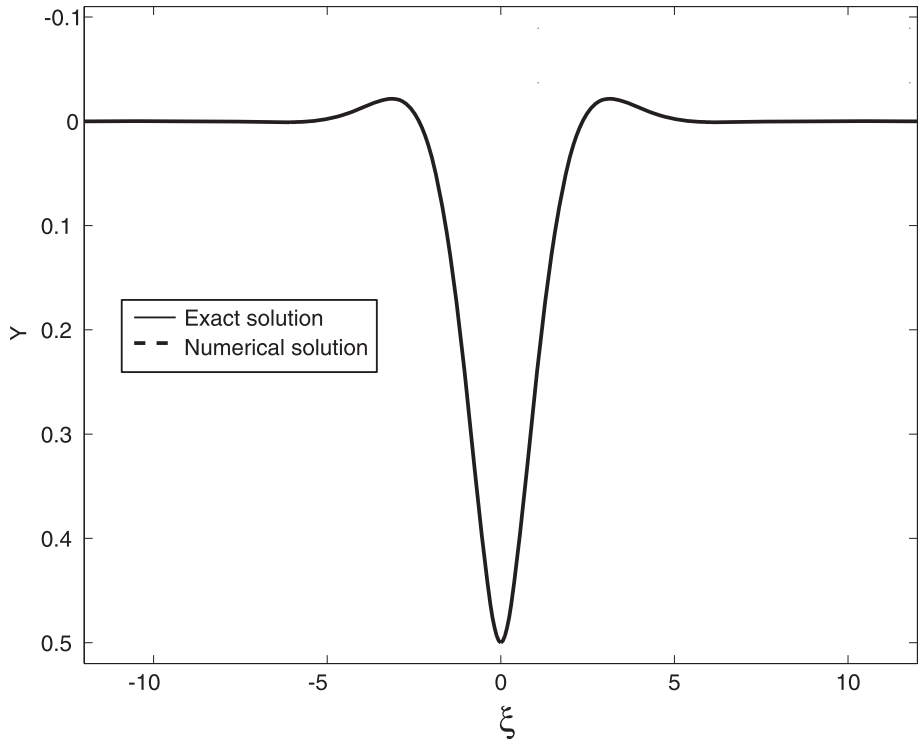

Fig. 3. Comparison of the analytical and numerical solutions of Eqs. (8) and (14) to the beam deflections on the Winkler foundation subjected to a concentrated load. The two solutions are almost identical.

bending in area $\mathbf{II}_1$ are clearly seen in Fig. 4. Fig. 5 shows the three beam deflections with $k_2/k_1 = 0$, $k_2/k_1 = 10^{-4}$ and $k_2/k_1 = 10^{-2}$. The $k_2/k_1 = 0$ case is the tensionless foundation. Their corresponding zero points of ξ_1s increase monotonically from $\pi/2$ to 1.67 and to 1.88 as k_2/k_1 increases. Similarly, the changes of three beam deflections are rather small around the area **I** center. Again, around the **I** edge and especially in the tensile area of $\mathbf{II}_1$, the differences of the three beam deflections are very significant. A smaller k_2/k_1 corresponds to a much larger defection. Computationally, we can easily reduce k_2/k_1 to, for example, 10^{-6}, to be closer to the limit case of $k_2/k_1 = 0$. However, the large deflection difference in the (tensile) area of $\mathbf{II}_1$ between the bi-linear foundation and the tensionless foundation models can only be

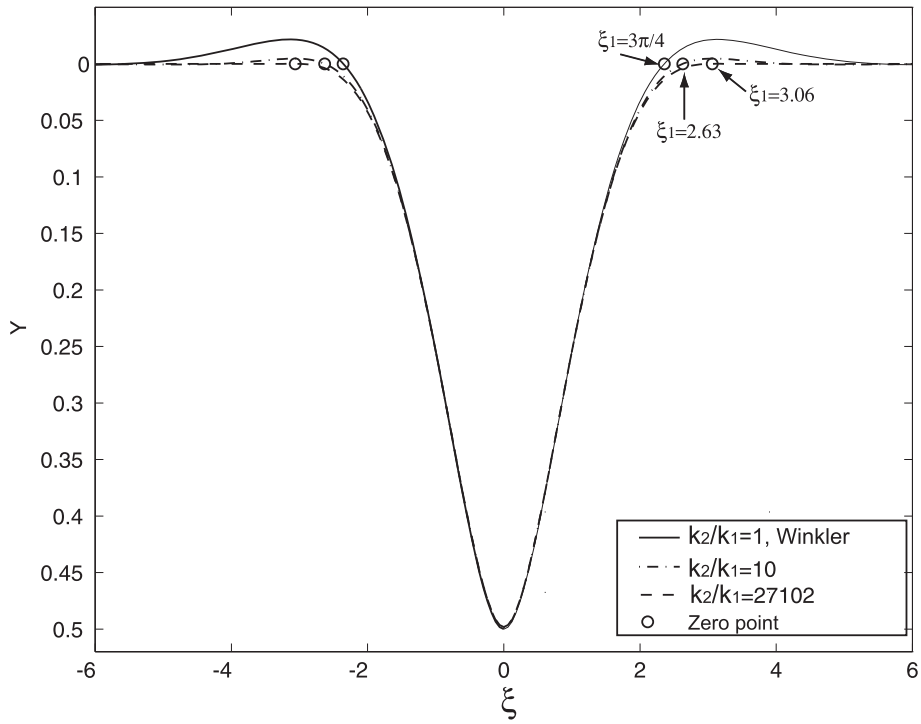

Fig. 4. The beam deflections with $k_2/k_1 = 1$, 10 and 27102, respectively. The corresponding first zero points are $\xi_1 = 3\pi/4$, 2.63 ($\approx 0.84\pi$) and 3.06 ($\approx 0.97\pi$), which increase monotonically with the increasing k_2/k_1.

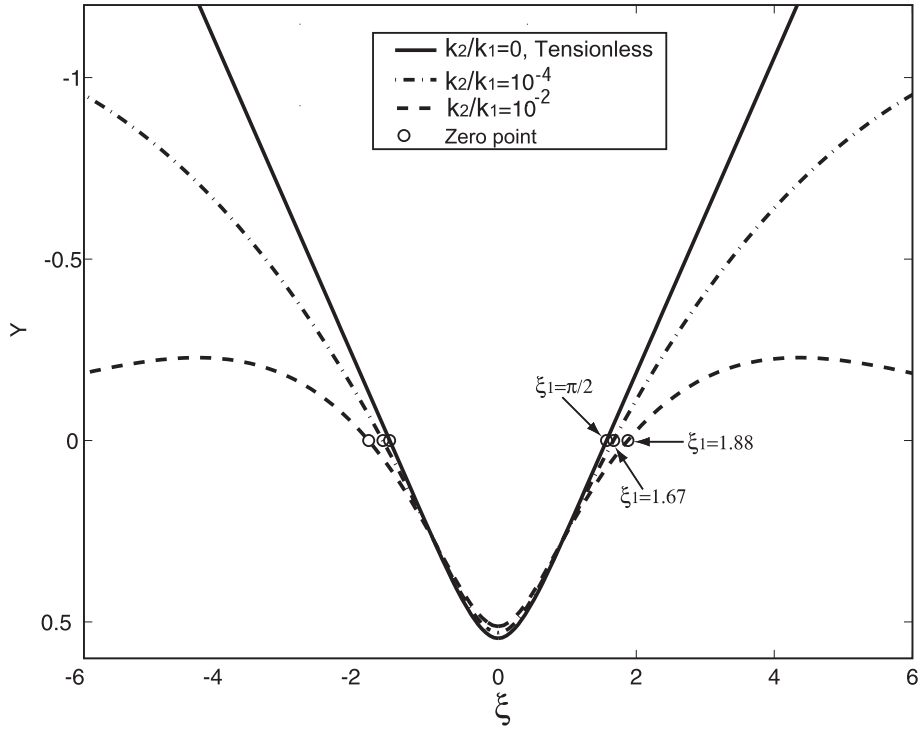

Fig. 5. The beam deflections with $k_2/k_1 = 0$, 10^{-4} and 10^{-2}, respectively. The corresponding first zero points are $\xi_1 = \pi/2$, 1.67 ($\approx 0.53\pi$) and 1.88 ($\approx 0.6\pi$), which also increase monotonically.

mildly reduced. For the tensionless foundation of Eq. (12), there is only one contact area and the beam deflection of the detachment part increases linearly to infinity. In contrast, the bilinear foundation with three zero-point assumption, $\lim_{\xi\to\infty} Y_{22}(\xi) = 0$ as seen in Eq. (14). Therefore, the assumed beam deflection by Eq. (14) is irreconcilable with that of the tensionless foundation, which is mainly responsible for the deflection difference in area $\mathbf{II}_1$. As the result, adding more zero points can only make the assumed beam deflection to deviate more from that of the tensionless foundation. The following computation is carried out by assuming one zero point and allowing the beam deflection to reach infinity, which mimics the beam deflection on the tensionless foundation to see if the problem can be mitigated. Now with only one zero point, the solution form to the bilinear foundations model becomes the following

$$\begin{cases} Y_1 = A_1 \sinh\xi \sin\xi + B_1 \cosh\xi \cos\xi - \frac{F}{2}\sinh\xi\cos\xi + \frac{F}{2}\cosh\xi\sin\xi, \mathbf{I} \\ \quad : 0 \le \xi \le \xi_1 \\ Y_{21} = C_{21} e^{R\xi}\sin(R\xi) + D_{21} e^{R\xi}\cos(R\xi), \mathbf{II}_1\text{: } \xi \ge \xi_1 \end{cases} \tag{19}$$

Notice that Y_{21} can reach infinity. Again, the five unknowns of A_1, B_1, C_{21}, D_{21} and ξ_1 can be solved by the four transversality conditions and one constraint condition at ξ_1. Fig. 6 shows the three beam deflections with $k_2/k_1 = 0$, $k_2/k_1 = 10^{-6}$ and $k_2/k_1 = 10^{-4}$. The three corresponding ξ_1s are now $\pi/2$, 1.54 and 1.47. In comparison with Fig. 5, as we the further reduce the k_2/k_1 ratio to 10^{-6}, its corresponding $\xi_1 = 1.54$ is also closer to the limit case of $\pi/2$. However, the beam deflection with $k_2/k_1 = 10^{-6}$ is still significantly different from that of the tensionless foundation. Mathematically, for the bilinear foundation, $Y_{21} = C_{21}e^{R\xi}\sin(R\xi) + D_{21}e^{R\xi}\cos(R\xi)$ of Eq. (19) is an oscillating function; for the tensionless foundation, $Y_2 = F/\sinh(\pi/2)(-\xi + \pi/2)$ of Eq. (12) is a monotonically decreasing linear function. Physically, $Y_{21}^{'} \neq 0$ and $Y_{21}^{''} \neq 0$ means that the beam bending moment and shear are not zero. Therefore, Y_{21} can not approach infinity without oscillation. Otherwise, the equilibrium cannot be satisfied. However, this bizarre and unphysical behavior of the beam deflection reaching infinity can never happen if the beam weight is considered (Weitsman, 1972). Furthermore, in the tensionless contact researches, the focuses are on the contact area rather than the deflection of the detachment parts (Weitsman, 1969, 1970, 1972). In that sense, as seen in both Figs. 5 and 6, our bilinear model has accurately captured the features of the tensionless contact inside area **I** when the k_2/k_1 is very small.

Fig. 7 shows the variations of the first three zero points as the functions of k_2/k_1, which is set in logarithmic scale. It is noticed that ξ_1 is a monotonically increasing function of k_2/k_1. At $\lg(k_2/k_1) = 0$, $\xi_1 = 3\pi/4$ corresponds to the Winkler foundation. As $\lg(k_2/k_1) \to -\infty$, ξ_1 approaches $\pi/2$ of the tensionless foundation; as $\lg(k_2/k_1) \to \infty$, ξ_1 approaches π. It is interesting to notice that when k_2/k_1 approaches $\pm\infty$, the corresponding ξ_1 is $\pi/4$ more/less than that of Winkler foundation. Both ξ_2 and ξ_3 are monotonically decreasing functions of k_2/k_1. Fig. 8 examines the above results from a different angle. As seen in Fig. 1(b), the contact lengths of area **I**, $\mathbf{II}_1$ and $\mathbf{III}_1$ are defined as $2\xi_1$, $\xi_2 - \xi_1$ and $\xi_3 - \xi_2$, respectively. These three contact lengths as the functions of k_2/k_1 are plotted in Fig. 8. The contact length of $2\xi_1$ monotonically increases. In contrast, the $\mathbf{II}_1$ contact length of $\xi_2 - \xi_1$ monotonically decreases, which approaches zero as $\lg(k_2/k_1) \to \infty$. As $\lg(k_2/k_1) \to \infty$, the k_2 spring acts as a rigid constraint to prevent the beam from bending upwards to form a tensile zone. This can also be clearly seen in Fig. 4: There is very little beam upward deflections in both the $k_2/k_1 = 10$ and $k_2/k_1 = 27102$ cases. When $\lg(k_2/k_1)$ is small, $\xi_2 - \xi_1$ is very large, which is also seen in Figs. 5 and 6. For the limit case of the tensionless foundation which corresponds to $\lg(k_2/k_1) = -\infty$, $\xi_2 - \xi_1$ becomes infinite and therefore, there is only one contact area.

4. Conclusion

For an infinite beam on a bilinear elastic foundation subjected to a concentrated load, a straightforward computational method is formulated. The computational method starts with assuming the number of zero points, giving the solution form to each area divided by the zero points and then solving them numerically by the Newton-Rhapson method. An arbitrary number of zero points, which also determines the

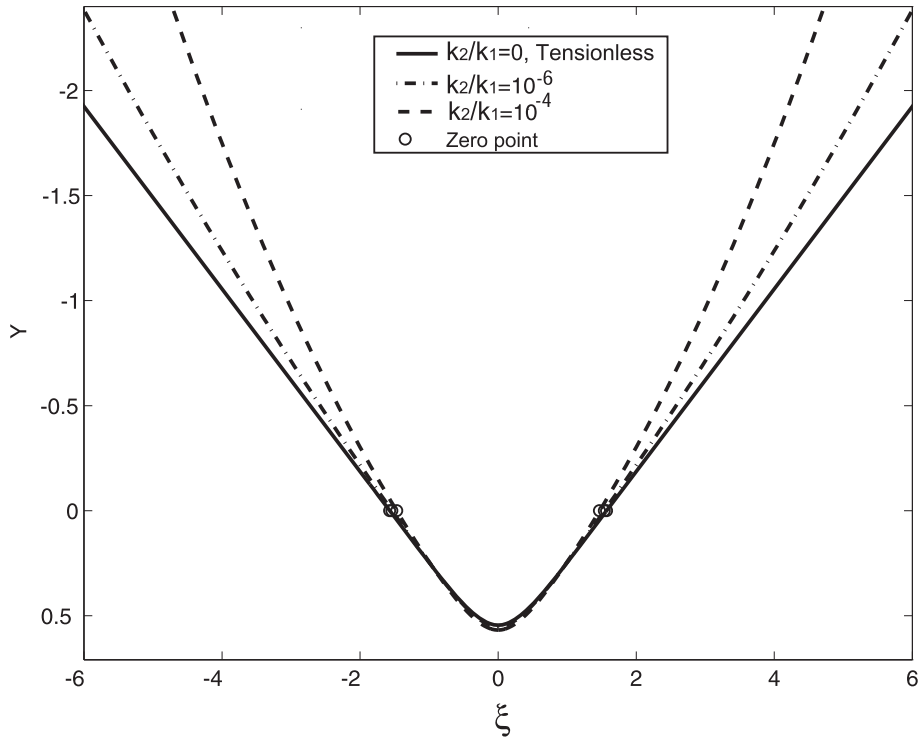

Fig. 6. The beam deflections with $k_2/k_1 = 0$, 10^{-6} and 10^{-4}, respectively. Compared with those in Fig. 5, there is only one zero point in the $\xi > 0$ area and $\lim_{\xi\to\infty} Y(\xi) = -\infty$. The corresponding first zero points are $\xi_1 = \pi/2$, 1.54 ($\approx 0.49\pi$) and 1.47 ($\approx 0.47\pi$), which decrease monotonically.

number of the unknowns, can be incorporated in the computational method. With a large number of the unknowns, the computation can be very time-consuming. The computations with the assumption of three zero points are shown to be very accurate when the ratio of two foundation moduli varies in a very large range. The physical mechanism for this accuracy is that the major deformations of both the elastic foundation and beam are in a small region around the concentrated load. The Winkler and tensionless foundations are the two special cases of this bilinear foundation: One reacts symmetrically to both tension and compression and the other reacts to compression only. With the bilinear elastic foundation model and the computational method developed in this study, a more general elastic foundation,

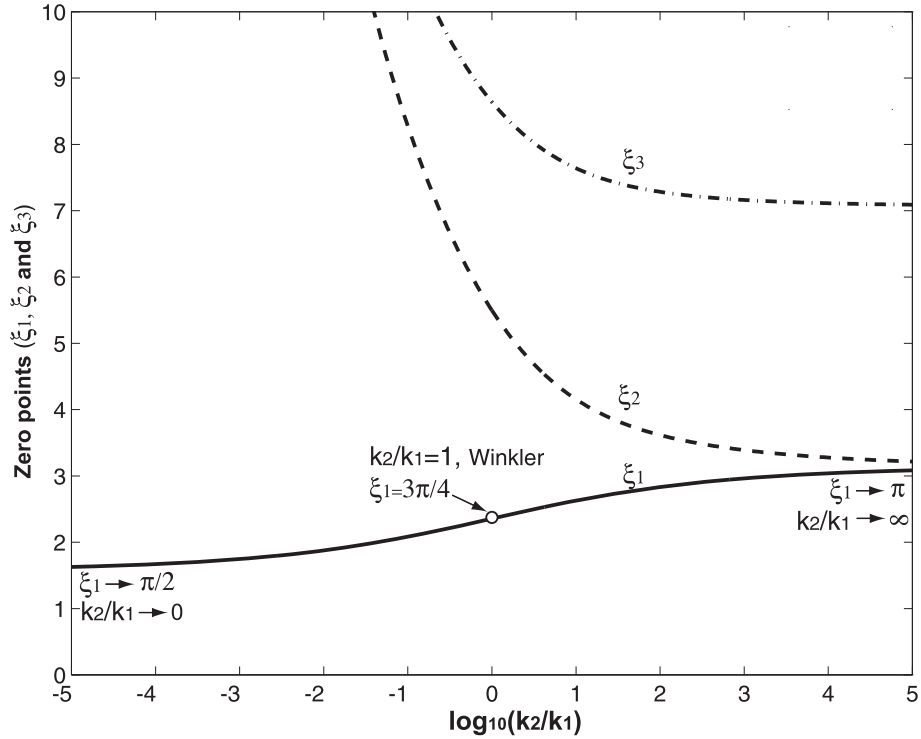

Fig. 7. The three zero points (ξ_1, ξ_2 and ξ_3) as the functions of $\lg(k_2/k_1)$. Here the zero points as seen in Fig. 1(b) are the locations at which the beam deflection is zero. $\lim_{k_2/k_1\to 0}\xi_1 = \pi/2$ is the limit case of the tensionless foundation and in comparison, $\lim_{k_2/k_1\to\infty}\xi_1 = \pi$. For the Winkler foundation of $k_2/k_1 = 1$, $\xi_1 = 3\pi/4$.

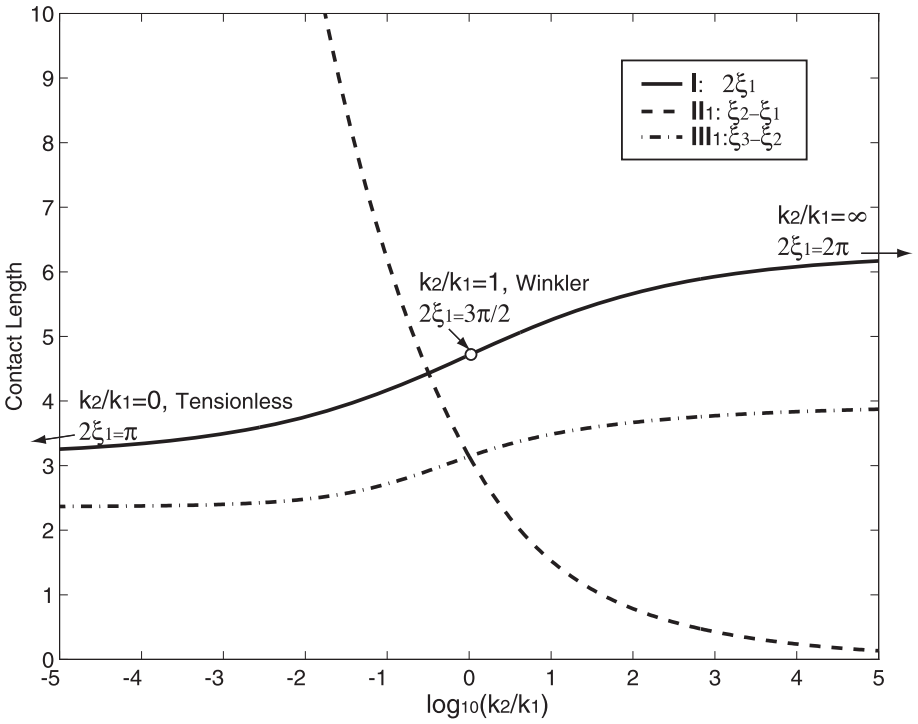

Fig. 8. The contact lengths as the functions of $\lg(k_2/k_1)$. For the areas of **I**, $\mathbf{II}_1$ and $\mathbf{III}_1$, the corresponding contact lengths are defined as $2\xi_1$, $\xi_2 - \xi_1$ and $\xi_3 - \xi_2$, respectively.

which reacts asymmetrically to tension and compression, can be efficiently handled. The independence of contact area(s) on a concentrated load is a benchmark property. The presence of a concentrated load only modifies the beam deflection. This independence property can be very helpful to the analysis and computation of the track deflection subjected to a concentrated load of track-wheel contact.

Acknowledgments

This work was supported by the National Natural Science Foundation of China (NSFC Nos. 11772335 and 11772334), the Strategic Program Research Program (B) of the Chinese Academy of Sciences (XDB22020201), the National Key Research and Development Program of China (2016YFB1200602-09 and 2016YFB1200602-10).

References

Ang, K.K., Dai, J., 2013. Response analysis of high-speed rail system accounting for abrupt change of foundation stiffness. J. Sound Vib. 332, 2954–2970.
Attar, M., Karrech, A., Regenauer-Lieb, K., 2016. Non-linear analysis of beam-like structure on unilateral foundations: a lattice spring model. Int. J. Solid Struct. 88–89, 192–214.
Bhattiprolu, U., Bajaj, A.K., Davies, P., 2013. An efficient solution methodology to study the response of a beam on viscoelastic and nonlinear unilateral foundation: static response. Int. J. Solid Struct. 50, 2328–2339.
Bhattiprolu, U., Davies, P., Bajaj, A.K., 2014. Static and dynamic response of beams on nonlinear viscoelastic unilateral foundations: a multimode approach. J. Vib. Acoust. 136, 031002.
Bhattiprolu, U., Bajaj, A.K., Davies, P., 2016. Periodic response predictions of beams on nonlinear and viscoelastic unilateral foundations using incremental harmonic balance method. Int. J. Solid Struct. 99, 28–39.
Bian, N., Jiang, H., Cheng, C., Chen, Y., Chen, R., Jiang, J., 2014. Full-scale model testing on a ballastless high-speed railway under simulated train moving loads. Soil Dynam. Earthq. Eng. 66, 368–384.
Biot, M.A., 1937. Bending of an infinite beam on an elastic foundation. J. Appl. Mech. 4, 1–7.
Brau, F., Vandeparre, H., Sabbah, A., Poulard, C., Boudaoud, A., Damman, P., 2011. Multiple-length-scale elastic instability mimics parametric resonance of nonlinear oscillations. Nat. Phys. 7, 56–60.
Choros, J., Adams, G., 1979. A steadily moving load on an elastic beam resting on a tensionless Winkler foundation. J. Appl. Mech. 46, 175–180.
Dempsey, J.P., Keer, L.M., Patel, N.B., Glasser, M.L., 1984. Contact between plates and unilateral supports. J. Appl. Mech. 55, 324–328.
Ebrahimi, F., Barati, M.R., 2017. Buckling analysis of nonlocal third-order shear deformable functionally graded piezoelectric nanobeams embedded in elastic medium. J. Braz. Soc. Mech. Sci. Eng. 39, 937–952.
Ebrahimi, F., Shaffiei, N., 2017. Influence of initial shear stress on the vibration behavior of single-layered graphene sheets embedded in an elastic medium on Reddy's higher-order shear deformation plate theory. Mech. Adv. Mater. Struct. 24, 761–772.
Farshad, M., Shahinpoor, M., 1972. Beams on bilinear elastic foundations. Int. J. Mech. Sci. 14, 441–445.
Heténi, M., 1946. Beams on Elastic Foundation. The University of Michigan Press.
Keer, L.M., Dundurs, J., Tsai, K.C., 1972. Problems involving a receding contact between a layer and a half space. J. Appl. Mech. 39, 1115–1120.
Kerr, A.D., 1964. Elastic and viscoelastic foundation models. J. Appl. Mech. 31, 491–498.
Kerr, A.D., 1972. The continuously supported rail subjected to an axial force and a moving load. Int. J. Mech. Sci. 14, 71–78.
Kerr, A.D., 1974. The stress and stability analyses of railroad tracks. J. Appl. Mech. 41, 841–848.
Kerr, A.D., 1976. On the derivation of well posed boundary value problems in structural mechanics. Int. J. Solid Struct. 12, 1–11Crossref.
Lancioni, G., Lenci, S., 2010. Dynamics of a semi-infinite beam on unilateral springs: touch-down points motion and detached bubbles propagation. Int. J. Non Lin. Mech. 45, 876–887.
Lin, L., Adams, G., 1987. Beam on tensionless elastic foundation. J. Eng. Mech. 113, 542–553.
Ma, X., Butterworth, J., Clifton, G., 2009a. Response of an infinite beam resting on a tensionless elastic foundation subjected to arbitrarily complex transverse loads. Mech. Res. Commun. 36, 818–825.
Ma, X., Butterworth, J., Clifton, G., 2009b. Static analysis of an infinite beam resting on a tensionless Pasternak foundation. Eur. J. Mech. Solid. 28, 697–703.
Ma, X., Butterworth, J., Clifton, G., 2011. Shear buckling of infinite plates resting on tensionless elastic foundations. Eur. J. Mech. Solid. 30, 1024–1027.
Nobili, A., 2013. Superposition principle for the tensionless contact of a beam resting on a Winkler or a Pasternak foundation. J. Eng. Mech. 139, 1470–1478.
Press, W.H., Flannery, B.P., Teukolsky, S.A., Vettering, W.T., 1986. Numerical Recipes. Cambridge University Press.
Shahwan, K.W., Waas, A.M., 1994. A mechanical model for the buckling of unilaterally constrained rectangular plates. Int. J. Solid Struct. 31, 75–87.
Silveira, R., Pereira, W., Goncalves, P., 2008. Nonlinear analysis of structural elements under unilateral contact constraints by a Ritz type approach. Int. J. Solid Struct. 45, 2629–2650.
Tran, M.T., Ang, K.K., Luong, V.H., 2014. Vertical dynamic response of non-uniform motion of high-speed rails. J. Sound Vib. 333, 5427–5442.
Tsai, N.C., Westmann, R.E., 1967. Beams on tensionless foundation. J. Eng. Mech. 93, 1–12.
Weitsman, Y., 1969. On the unbonded contact between plates and an elastic half space. J. Appl. Mech. 36, 505–509.
Weitsman, Y., 1970. On foundations that react in compression only. J. Appl. Mech. 37,

1019–1030.
Weitsman, Y., 1971. Onset of separation between a beam and tensionless elastic foundation under a moving load. Int. J. Mech. Sci. 13, 707–711.
Weitsman, Y., 1972. A tensionless contact between a beam and an elastic half-space. Int. J. Eng. Sci. 10, 73–81.
Zhang, Y., Murphy, K.D., 2004. Response of a finite beam in contact with a tensionless foundation under symmetric and asymmetric loading. Int. J. Solid Struct. 41, 6745–6758.
Zhang, Y., 2008. Tensionless contact of a finite beam resting on Reissner foundation. Int. J. Mech. Sci. 50, 1035–1041.
Zhang, Y., Murphy, K.D., 2013. Tensionless contact of a finite beam: concentrated load inside and outside the contact zone. Acta Mech. Sin. 29, 836–839.
Zhuo, L., Zhang, Y., 2015a. The Mode-coupling of a stiff film/compliant substrate systems in the post-buckling range. Int. J. Solid Struct. 53, 28–37.
Zhuo, L., Zhang, Y., 2015b. From period-doubling to folding in stiff film/soft substrate system: the role of substrate nonlinearity. Int. J. Non Lin. Mech. 76, 1–7.